S. C. Chapman, P. T. Lang, R. O. Dendy, L. Giannone, N. W. Watkins and ASDEX Upgrade Team

Control system-plasma synchronization and naturally occurring edge localized modes in a tokamak

Article (Published version) (Refereed)

Control system-plasma synchronization and naturally occurring edge localized modes in a tokamak

S. C. Chapman, P. T. Lang, R. O. Dendy, L. Giannone, N. W. Watkins, and ASDEX Upgrade Team

Citation: Physics of Plasmas **25**, 062511 (2018); doi: 10.1063/1.5025333
View online: https://doi.org/10.1063/1.5025333
View Table of Contents: http://aip.scitation.org/toc/php/25/6
Published by the American Institute of Physics

Control system-plasma synchronization and naturally occurring edge localized modes in a tokamak

S. C. Chapman,[1,2,a)] P. T. Lang,[3] R. O. Dendy,[1,4] L. Giannone,[3] N. W. Watkins,[1,2,5,6] and ASDEX Upgrade Team[2]

EUROfusion Consortium, JET, Culham Science Centre, Abingdon, United Kingdom
[1]*Centre for Fusion, Space and Astrophysics, Department of Physics, University of Warwick, Coventry CV4 7AL, United Kingdom*
[2]*Center for Space Physics, Department of Astronomy, Boston University, Boston, Massachusetts 02215, USA*
[3]*Max-Planck-Institut für Plasmaphysik, Tokamak Scenario Development Division (E1), Boltzmannstrasse 2, 85748 Garching, Germany*
[4]*CCFE, Culham Science Centre, Abingdon, Oxfordshire OX14 3DB, United Kingdom*
[5]*Centre for the Analysis of Time Series, London School of Economics and Political Science, London WC2A 2AE, United Kingdom*
[6]*School of Science, Technology, Engineering and Mathematics, Open University, Milton Keynes MK7 6AA, United Kingdom*

(Received 8 February 2018; accepted 7 June 2018; published online 26 June 2018)

Edge Localised Modes (ELMs) naturally occur in tokamak plasmas in high confinement mode. We find in ASDEX Upgrade that the plasma can transition into a state in which the control system field coil currents, required to continually stabilize the plasma, continually oscillate with the plasma edge position and total MHD energy. These synchronous oscillations are one-to-one correlated with the occurrence of natural ELMs; the ELMs all occur when the control system coil current is around a specific phase. This suggests a phase synchronous state in which nonlinear feedback between plasma and control system is intrinsic to natural ELMing, and in which the occurrence time of a natural ELM is conditional on the phase of the control system field coil current.
https://doi.org/10.1063/1.5025333

I. INTRODUCTION

Large-scale tokamak experiments self-organise to generate large scale structures and flow with enhanced confinement, known as H-mode.[1] Edge localized modes.[2–5] (ELMs) are intense, short duration relaxation events observed in tokamak H-mode regimes. Typically, in present day devices, a few hundred ELMs occur naturally in the quasi-stationary phase of H-mode plasmas. Each ELM releases particles and energy which load the plasma facing components; scaled up to ITER,[6] the largest such loads are unacceptable.[7,8] ELMs are also a key in removing plasma impurities which must be achieved in a controllable manner. Thus, ELM prediction, mitigation, and control[9–20] are central to MCF research. The peeling-ballooning MHD instability of the plasma edge is believed to underlie ELM initiation.[21–23] However, a fully comprehensive model for the birth-to-death ELM cycle is not yet available. These large-scale experiments exhibit nonlinear coupling of plasma physics processes over several orders of magnitude in spatio-temporal scale. A ubiquitous aspect of such strongly connected, many component physical systems is the potential for self-organisation to synchronous states where nonlinear active feedback between global and local scales leads to emergent global dynamics.[24–26]

Active control of the plasma is required to automatically maintain a global steady state and this is achieved by the control system's real-time monitoring of the plasma (Ref. 27 and references therein). The control system takes a variety of inputs, and one of its automatic, internally generated outputs is to apply voltages to field coils that regulate the vertical plasma position (vertical stabilization control coils, see Fig. 1 of Ref. 28). The applied voltages modify the currents in the field coils, generating inductive magnetic fields that react back on the plasma. In the standard paradigm for the natural ELM cycle, the control system is constantly active by stabilizing the plasma and simply acts on a relatively short timescale to restore the plasma steady state following an ELM. The control system is not a part of standard physical models for the ELM cycle. A new hypothesis[29–32] is that phase coherent nonlinear feedback between the plasma and the automatic control system is part of the observed natural ELM cycle. Importantly, this phase coherent feedback which we propose here is distinct from a scenario, whereby the control system causes ELMs by direct destabilisation, and from the entrainment of triggered ELMs by externally applied vertical magnetic kicks[9–12] which relies on kicks of sufficiently large amplitude, typically much larger than that seen in the control system vertical field coil current during natural ELMing. Phase coherent feedback in natural ELMing is found on JET[29–32] in which the occurrence time of natural ELMs can be conditioned by the phase, rather than the amplitude, of the control system and global plasma dynamics. If such a relationship exists between the control system and naturally occurring ELMs, then we would anticipate that under certain conditions the coupled control system and

[a)]Electronic mail: S.C.Chapman@warwick.ac.uk

plasma dynamics governing natural ELM occurrence can access a state in which they are fully phase synchronized.[24] We report the observation of just such a dynamics here and discuss the physical context with a simple example of phase synchronization.

II. DETAILS OF THE TIME SERIES ANALYSIS

We focus on global signals that are all at high time resolution ($\simeq 50$ ms), examples of which are shown in Fig. 1 for an interval of synchronous dynamics. The time series will be plotted in this format throughout, and the panels from top to bottom are: (i) the location of the outboard edge of the plasma (R_{out}), (ii) an ELM monitor from which we identify the ELM occurrence times, (iii) total magnetohydrodynamic field and plasma stored energy (W_{MHD}), (iv) the current in the upper (I_C^u) and lower (I_C^l) field coils (I_C^u time series are shown), which are actively used for vertical stabilization of the plasma by the control system (vertical stabilization control coils, see Fig. 1 of Ref. 28) (v) its instantaneous phase, and (vi) the line averaged plasma density ($\bar{n}_e$). We are concerned with the temporal phase of this vertical field coil current.

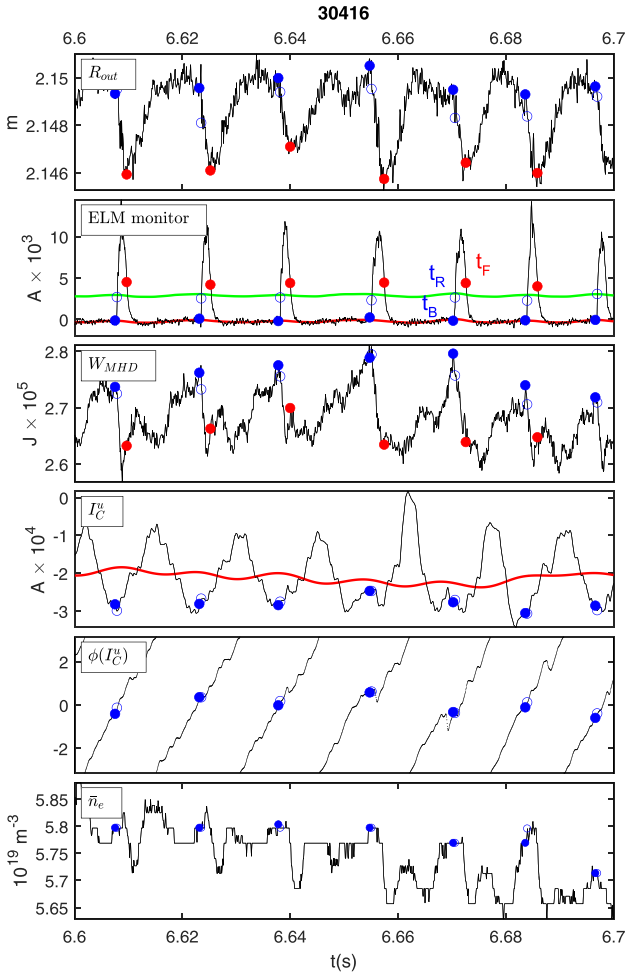

FIG. 1. Time traces plotted for a short time window within interval $t = 6.4$ s–7.1 s of synchronous dynamics in plasma 30416 showing one-to-one correlation between ELM occurrence and vertical control system current temporal phase. From top to bottom (black traces): the edge position (R_{out}); the ELM monitor; the total plasma MHD energy (W_{MHD}); the current in the upper vertical control system coil (I_C^u); its analytic temporal phase ($\phi(I_C^u)$); and the averaged plasma density ($\bar{n}_e$). Filled blue circles are at times for all the ELMs just before the start of each ELM crash, $t_B = t_R - 0.35$ ms, where t_R is the ELM onset time. Additional times determined from the ELM monitor signal are also plotted: the ELM onset time t_R (open blue circles) and end time t_F (filled red circles) at the ELM monitor signal upcrossing and downcrossing of a threshold (green line) one standard deviation away from the running baseline (red line) of the ELM monitor signal. The ELM monitor signal for one ELM is annotated with times t_B, t_R, and t_F for clarity. This short time interval is indicated by the red bar in Fig. 3 top panel.

The ELM monitor signal performs a steep rise at the start of each natural ELM from which we can identify an ELM onset time. The ELM can also be identified by the steep drop in plasma stored energy W_{MHD} and sharp inward movement of the plasma outboard edge R_{out}. We can apply a simple algorithm across the entire timeseries to identify the time just before the ELM, at which the stored energy W_{MHD} and outboard edge R_{out} are both at peak values just before the ELM. We determine the ELM occurrence times from the ELM monitor signal using an algorithm as follows (Fig. 1 second from top panel). We find a 300 pt (0.015 s) locally weighted regression (LOESS) running mean $R(t)$ which down-weights outliers (red line). We then subtract this running mean from the ELM monitor signal $I(t)$ giving $S(t) = I(t) - R(t)$. We select as a threshold $TH(t)$ the running mean plus one standard deviation of $S(t)$ (green line). ELM onsets can be seen at the time when the ELM monitor is sharply rising which we identify as time t_R (of the data point before) the first up-crossing time when $S(t) > TH(t)$ (open blue circles). The end of the ELM crash is identified as the time when the ELM monitor falls below the same threshold at time t_F (of the data point before) the first down crossing time $S(t) < TH(t)$ following the ELM monitor peak, (filled red circles). To test the idea that the control system is in continual feedback with the plasma-ELMing process and so influences ELM onset, as well as responding to ELM crash, we also identify a time t_B just before the beginning of the ELM. We find that a single value of the time interval dt used to define $t_B = t_R - dt$, when applied to both these plasmas, can quite closely identify the time just before the ELM monitor trace performs a steep rise at ELM onset. From Fig. 1, we can see that t_B also quite closely identifies the time where the MHD energy is maximal, and where the plasma edge position R_{out} is at a peak value just before each ELM crash (times t_B are shown as filled blue circles on the plots). Throughout we will use $dt \simeq 0.35$ ms or 7 data points. To avoid detection of multiple crossings due to noise, $S(t)$ is a 5 point running average of the original signal and we exclude multiple crossings within 50 data points of each other.

The control system field coil current instantaneous phase $\phi(I_C^u)$ is obtained from the analytic signal $S(t) + iH(t) = A\exp[i\phi(t)]$ ($H(t)$ is the Hilbert transform of $S(t)$). This defines an instantaneous temporal analytic amplitude $A(t)$ and phase $\phi(t) = \omega(t)t$. We compute the analytic signal by Hilbert transform over the entire plasma flat top after removing the time-varying baselines of the $I_C^{u,l}$ by subtracting a 1000 pt running LOESS mean (red line in Fig. 1). Baseline removal is required in order to obtain positive instantaneous frequency, that is, time increasing analytic phase from the Hilbert transform for the characteristic signal oscillations. Provided that the signal crosses the baseline on each such oscillation, the analytic phase is insensitive to the details of

the baseline. Phases are given relative to the average $\langle\phi(t_B)\rangle$ over all ELMs in the interval.

III. OVERVIEW OF INTERVALS OF SYNCHRONOUS DYNAMICS IN PLASMAS 30416 AND 30930

We present here two examples of intervals of synchronous dynamics in the steady state H-mode flat-top of ASDEX Upgrade plasmas 30416 and 30930. We have[33] briefly discussed an example in another ASDEX-Upgrade plasma, 30792, which had parameters: $I_P = 0.8\,\mathrm{MA}$, $B_t = -2.5\,\mathrm{T}$, $\bar{n}_e \sim 6.7 \times 10^{19}\mathrm{m}^{-3}$, neutral beam injection heating (NBI) $P_{NBI} = 2.5\,\mathrm{MW}$, and electron cyclotron resonant heating (ECRH) of 1.3 MW. An estimate of the ELM frequency from the average inter-ELM time interval over the time intervals of synchronous dynamics gives $66.7\,\mathrm{s}^{-1}$ and $80\,\mathrm{s}^{-1}$ for plasma 30416 and plasma 30930, respectively. The change in conditions that coincides with the transition to synchronous dynamics is different for these two cases.

A. Plasma 30416 overview and time domain behaviour

Figure 2 gives an overview of this plasma which has parameters $I_p = 0.8\,\mathrm{MA}, B_T = 2.5\ \mathrm{T}, P_{NBI} = 2.5\,\mathrm{MW}$, and $n_e \sim 5.7 \times 10^{19}\mathrm{m}^{-3}$. Electron cyclotron resonant heating (ECRH) of 1.2 MW at 140 GHz ends at $t = 6.2\,\mathrm{s}$. At the time of the ECRH switch-off, the total MHD energy drops by about 6% and we then see a transition to a synchronous state; this dynamics persists until $t \simeq 7.1\,\mathrm{s}$, after which the plasma terminates. This transition is shown in more detail in Fig. 3, and Fig. 1 shows a short (0.1 s) time interval of synchronous dynamics. The natural ELM crash generates a sharp drop in total plasma energy (W_{MHD}) and an inward movement of the plasma edge (R_{out}). Following the transition to synchronous dynamics at $t \simeq 6.2\,\mathrm{s}$, we can see that at times t_B (filled blue circles) the I^u_C current temporal phase of its oscillatory behaviour is around the same value (zero, phases are plotted w.r.t. the average). This time t_B is where the W_{MHD} and R_{out}

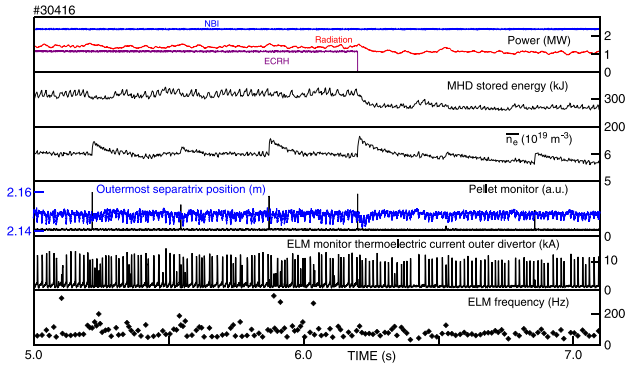

FIG. 2. Experimental plasma parameters for the latter part of plasma 30416. Top panel: Neutral beam injection (NBI) heating (blue line) and plasma radiation (red line) are constant. Electron cyclotron resonant heating (ECRH, purple line) is stepped down at $t = 6.2\,\mathrm{s}$. Second panel: Total MHD stored energy which drops at ECRH switch-off. Third panel: Line averaged plasma density which is enhanced on pellet injection. Fourth panel: Pellet monitor spikes identify pellet times. Fifth panel: ELM monitor (blue line) from which we identify the ELM occurrence times as the rise in the thermoelectric current observed at a tile in the divertor region, and pellet monitor (black line) and sixth panel: ELM frequency.

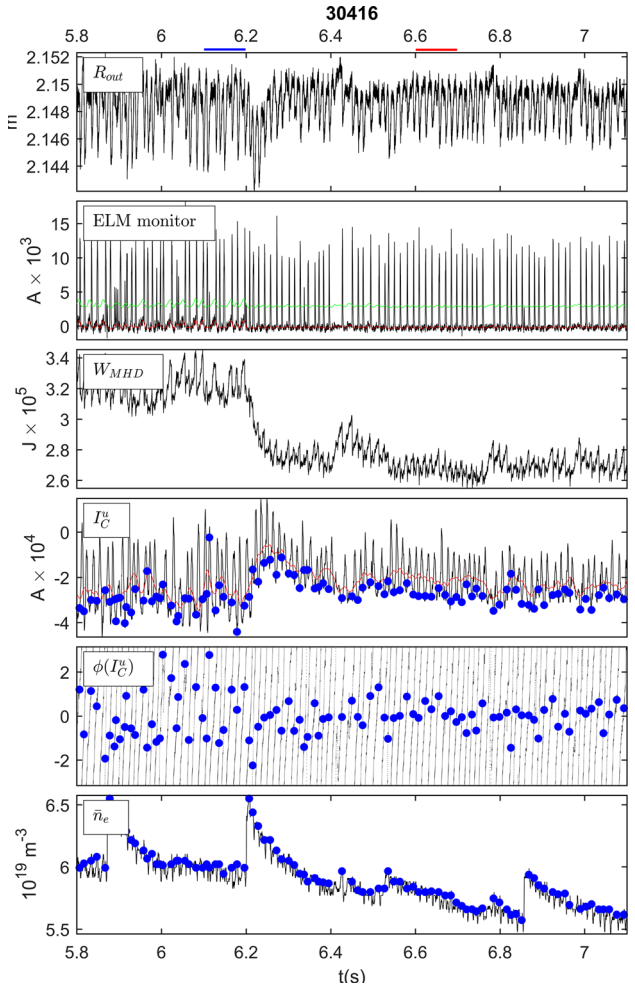

FIG. 3. Vertical control system current temporal phase just before each natural ELM becomes localised by following the transition to synchronous dynamics which occurs after $t \simeq 6.2\,\mathrm{s}$ in plasma 30416. The format of the plot is a simplified version of that of Fig. 1. From top to bottom (black traces): the edge position (R_{out}); the ELM monitor; the total plasma MHD energy (W_{MHD}); the current in the upper vertical control system coil (I^u_C); its analytic temporal phase ($\phi(I^u_C)$); and the averaged plasma density ($\bar{n}_e$). Filled blue circles are at times for all the ELMs just before the start of each ELM crash, $t_B = t_R - 0.35\,\mathrm{ms}$, where t_R is the ELM onset time.

are locally at peak values just before each natural ELM occurs (rise in the ELM monitor and sharp drop in W_{MHD} and R_{out}). Before the ECRH heating switch-off, they occur over a broad range of $\phi(I^u_C)$. This synchronous dynamics persists, whilst two pellets are injected during this interval, one of which enhances the line averaged plasma density ($\bar{n}_e$) by about 7%. For comparison, Fig. 4 plots a short time interval before the transition to synchronous dynamics; it is of the same time duration (0.1 s), and in the same format, as Fig. 1.

B. Plasma 30930 overview and time domain behaviour

Figure 5 gives an overview of this plasma which has parameters $I_p = 0.8\,\mathrm{MA}, B_T = 2.5\,\mathrm{T}, P_{NBI} = 2.3\,\mathrm{MW}$, and $\bar{n}_e \sim 6.2 \times 10^{19}\,\mathrm{m}^{-3}$. Electron cyclotron resonant heating of 1.8 MW at 140 GHz ends at $t = 8.0\,\mathrm{s}$. An overview plot in the same format as Fig. 3 is given in Fig. 6. From $t = 2.0$–$2.6\,\mathrm{s}$, there is a shift in plasma position, and just after the plasma has passed the maximum shift in R_{out} we see

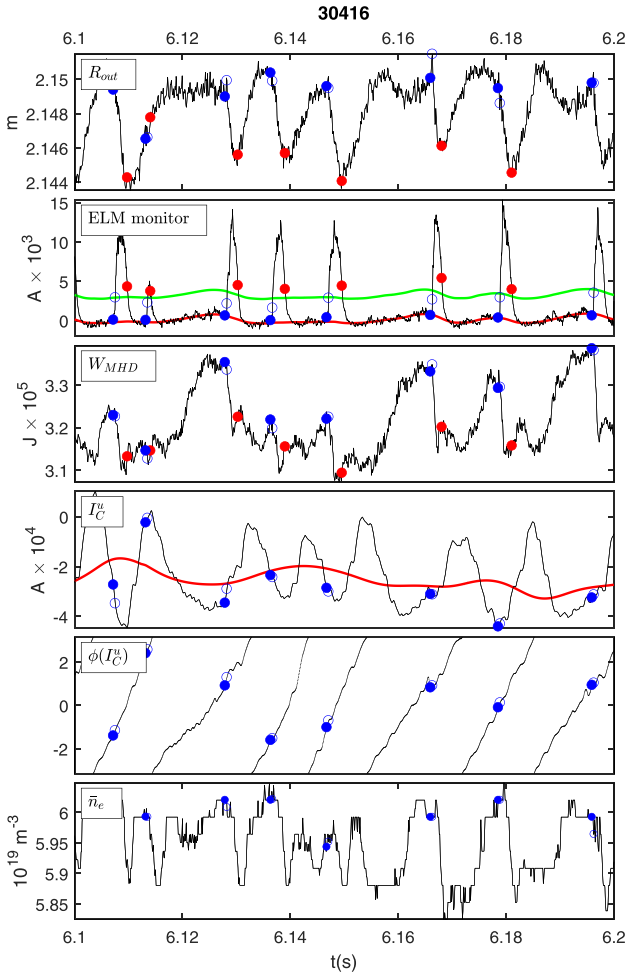

FIG. 4. Time traces plotted for a 0.1 s time window (of the same duration as in Fig. 1) at a time before the transition to synchronous dynamics in plasma 30416. Format is as in Fig. 1. This short time interval is indicated by the blue bar in Fig. 3 top panel.

a transition to synchronous dynamics at about $t = 2.35$ s. The synchronous dynamics ends after $t = 2.7$ s where there is a NBI beam dropout with corresponding drop in W_{MHD}; following this there is a sequence of injected pellets that modify the plasma, the first of these can be seen to enhance the line averaged plasma density ($\bar{n}_e$) by about 3%–4%.

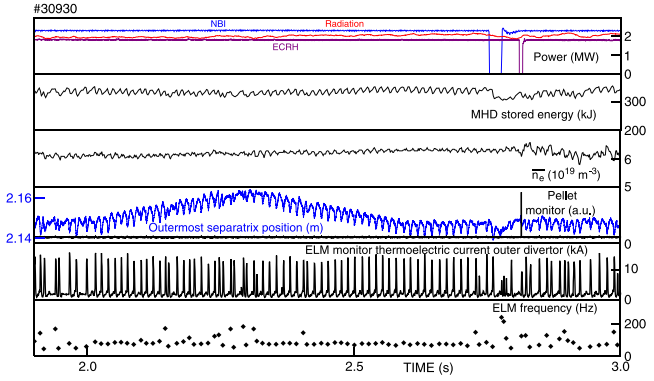

FIG. 5. Experimental plasma parameters for the early part of plasma 30329, in the same format as Fig. 2. The plasma position is shifted during $t = 2.0$–2.6 s and at $t = 2.75$ s, the NBI beam drops shortly, changing the heating. Following this is the first of a sequence of injected pellets.

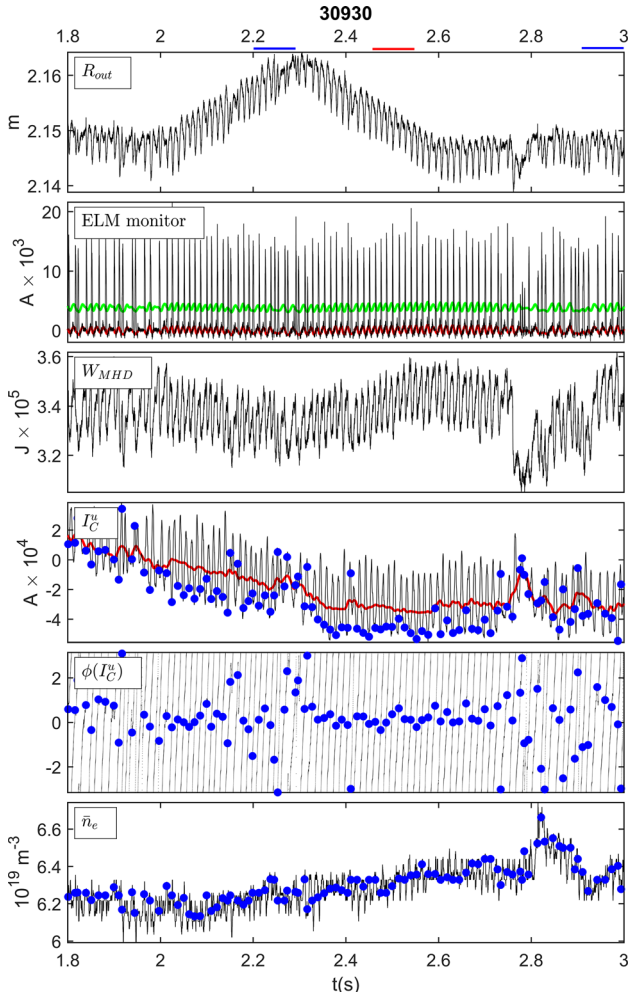

FIG. 6. Vertical control system current temporal phase just before each natural ELM becomes localised by following the transition to synchronous dynamics which occurs between $t \simeq 2.35$–2.7 s in plasma 30930. The format of the plot is a simplified version of that of Fig. 1; from top to bottom (black traces): the edge position (R_{out}); the ELM monitor; the total plasma MHD energy (W_{MHD}); the current in the upper vertical control system coil (I_C^u); its analytic temporal phase ($\phi(I_C^u)$); and the averaged plasma density ($\bar{n}_e$). Filled blue circles are at times for all the ELMs just before the start of each ELM crash, $t_B = t_R - 0.35$ ms, where t_R is the ELM onset time.

More detailed plots are given in Figs. 7–10 which are plotted in the same format as Fig. 1. Figure 7 plots the full time interval $t = 2.35$–2.7 s of synchronous dynamics. We can see that again, at time t_B (filled blue circles) the I_C^u current temporal phase of its oscillatory behaviour is found to be around the same value (zero, phases are plotted w.r.t. the average) when the W_{MHD} and R_{out} are locally at peak values just before each natural ELM occurs (rise in the ELM monitor and sharp drop in W_{MHD} and R_{out}). Plots of short (0.1 s) intervals are given to provide a comparison of the synchronous dynamics (Fig. 8) and the behaviour at times before (Fig. 9) and after (Fig. 10) in plasma 30930.

IV. STATISTICAL QUANTIFICATION OF PHASE ALIGNMENT

We now quantify the level of phase bunching. The temporal analytic phase at which each *kth* ELM occurs ϕ_k defines a unit magnitude complex variable $\underline{r}_k = e^{i\phi_k}$. A

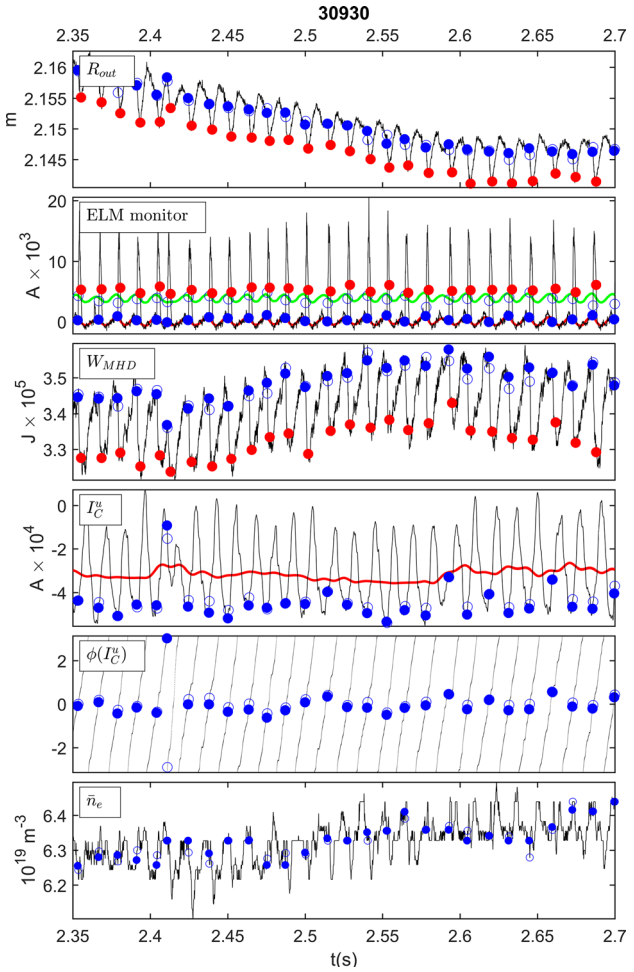

FIG. 7. Time traces plotted for the full time interval $t = 2.35$–2.7 s of synchronous dynamics in plasma 30930. Format is as in Fig. 1.

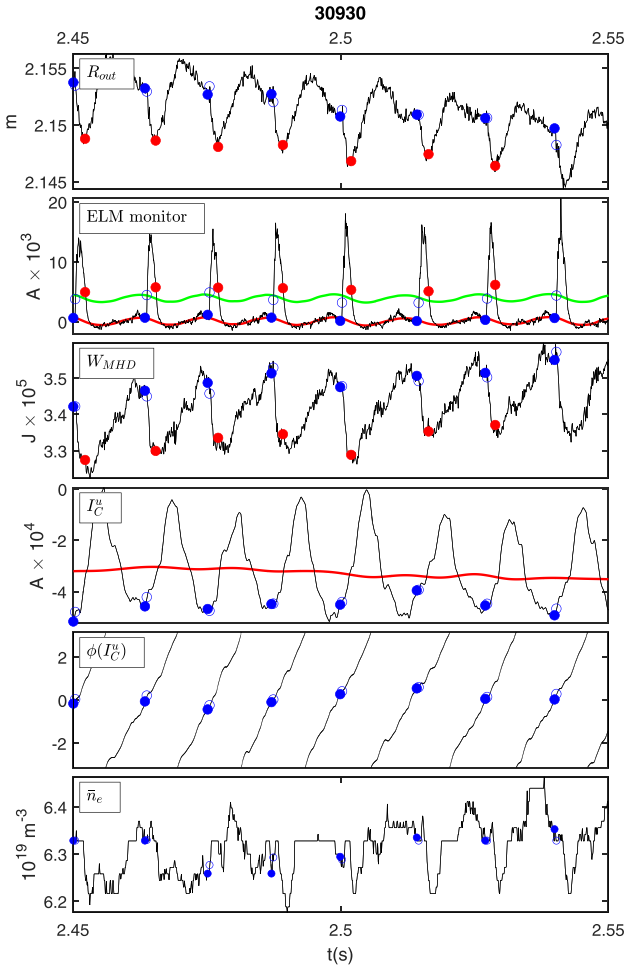

FIG. 8. Time traces plotted for a short time window of the same duration as in Fig. 1 at a time within the interval of synchronous dynamics in plasma 30930. Format is as in Fig. 1. This short time interval is indicated by the red bar in Fig. 6 top panel.

measure of phase alignment is the magnitude of the vector sum, normalized to N, the Rayleigh number: $R = \frac{1}{N}|\sum_{k=1}^{N} \underline{r}_k|$ If $R = 1$, the temporal phases are completely aligned. An estimate of the p-value under the null hypothesis that the vectors are uniformly distributed around the circle is:[34] $p = \exp[\sqrt{1 + 4N + 4N^2(1 - R^2)} - (1 + 2N)]$; a small value of p indicates significant departure from uniformity, i.e., the null hypothesis can be rejected with 95% confidence for $p < 0.05$.

Figures 11 and 12 (left panels) plot histograms of the I_C^u and I_C^l phases at all natural ELM occurrence times for time intervals of synchronous dynamics in plasmas 30416 and 30329, respectively. For comparison (right panels), we also plot histograms for all ELMs occurring in intervals of equal duration at times outside of the intervals identified with synchronous dynamics. Statistics are shown for the phases at the ELM onset times (upper panel, t_R) and just before the ELM (lower panel, t_B); we calculate Rayleigh's R at both these times. In both plasmas 30416 and 30329, we observed $R > 0.85$ for ELMs occurring in time intervals of synchronous dynamics ($p < 10^{-5}$ for all cases of synchronized dynamics) for the upper field coil current I_C^u. The lower field coil current I_C^l is at antiphase to that in I_C^u and shows the same level of phase bunching in 30329 and slightly weaker phase bunching in 30416. These field coils interact with the plasma in a manner that does not vary toroidally and in this sense act to modify global plasma dynamics. Importantly, we see equally strong phase synchronization when each ELM onset has begun and at a time before it; thus, this phase relationship is not simply due to the response of the control system to each ELM crash, and it involves the active feedback between control system and plasma that is constantly occurring. For comparison, at times outside of the intervals identified with synchronous dynamics (right panels) plots, these we find $R < 0.4$ and $R < 0.25$ for I_C^u and I_C^l, respectively.

V. SYNCHRONOUS DYNAMICS

Figures 13 and 14 show the synchronized dynamics of control system and plasma. These plots are constructed for the intervals of synchronous dynamics $t = 6.4$ s to 7.1 s in plasma 30416 and $t = 2.35$ s to 2.7 s in plasma 30930. In each of these figures, the left hand panels plot the running mean subtracted location of the plasma outer edge $R_{out} - \langle R_{out} \rangle$ and the total plasma MHD energy $W_{MHD} - \langle W_{MHD} \rangle$ versus the (running mean subtracted) current in the control system field coils $I_c^u - \langle I_c^u \rangle$ for the interval where there is

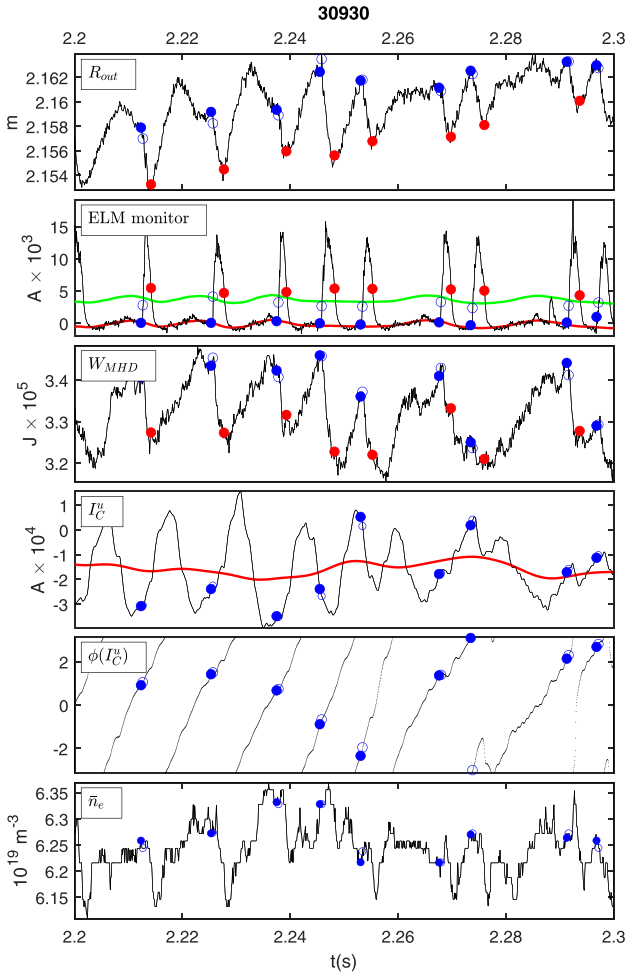

FIG. 9. Time traces plotted for a short time window of the same duration as in Fig. 1 at a time before the interval of synchronous dynamics in plasma 30930. Format is as in Fig. 1. This short time interval is indicated by the first blue bar in Fig. 6 top panel.

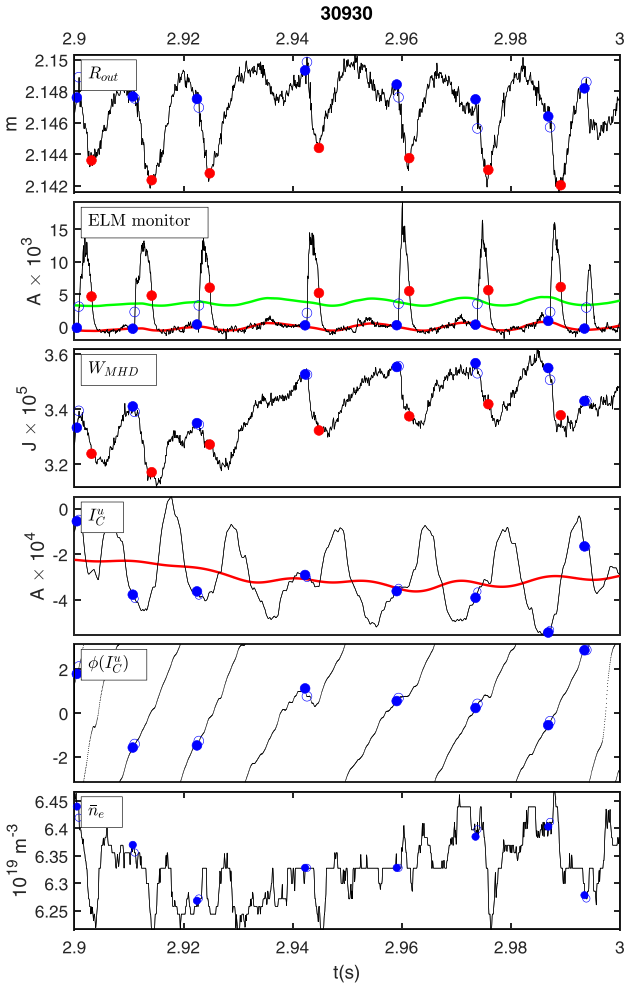

FIG. 10. Time traces plotted for a short time window of the same duration as in Fig. 1 at a time after the interval of synchronous dynamics in plasma 30930. Format is as in Fig. 1. This short time interval is indicated by the second blue bar in Fig. 6 top panel.

synchronous dynamics. Blue circles plot the signal values just before each ELM, at time t_B. For each ELM, the plasma and control system together execute a cycle: (a) there is a build up during which the plasma total energy increases with little change in the outer edge location, whilst the current in the control system coils becomes more negative followed by (b) the ELM crash, in which both the total energy sharply drops and the plasma edge moves rapidly inward, whilst the control system current does not change significantly then (c) a recovery in which the control system becomes more positive, the plasma edge moves outwards and the total energy at first does not change significantly. The control system field coil current (I_C^u) phase orders the global plasma dynamics as captured by the total plasma energy and edge location; the right hand panels plot these quantities versus I_C^u signal phase. Just before the ELM onset, at time t_B (blue circles) the I_C^u phases are clustered about zero and we can see that the build up (a) and recovery (c) occur over two halves ($[-\pi, 0]$ and $[0, \pi]$) of the (I_C^u) control system current cycle. This synchronous dynamics can be quite stable, the synchronous dynamics in plasma 30416 persists, whilst an injected pellet enhances the line averaged plasma density $\bar{n}_e$ by about 7%.

VI. DISCUSSION

There are several possible physics scenarios that could generate this observed phase coherent dynamics and to differentiate them we discuss some examples here. The suggestion that in natural ELMing "the control system and plasma [is] behaving as a single nonlinearly coupled system, rather than as driver and response" was first made by some of the present authors in the context of JET.[29] In these JET plasmas, we found that the phase of toroidal full flux loop signals became aligned around a single value just before the onset of each natural ELM.[29–32] In particular,[30] we found a class of prompt natural ELMs which are at distinct short inter-ELM time intervals that occur at a specific phase of the plasma's own response to the previous ELM. For these ELMs, the initial ELM and its successor form a linked pair, in that the second ELM arises near the end of the first. We would thus expect under some plasma conditions a global dynamics in which *all* the ELMs are "prompt," with each ELM directly following the previous one. We have identified just such a dynamics here on ASDEX Upgrade in which the excursions of the control system and perturbations in the plasma are completely phase synchronized,[24–26] with their synchronous

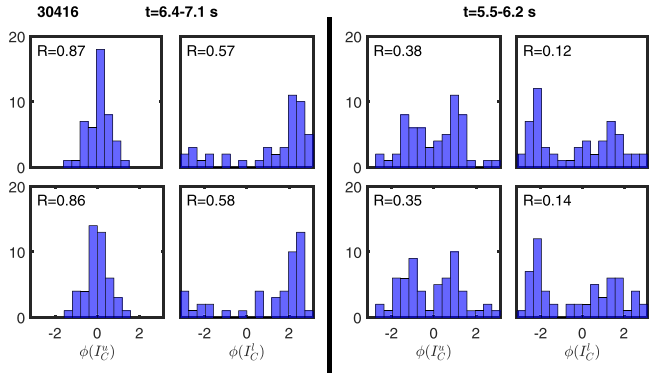

FIG. 11. Each set of four panels plots histograms of instantaneous temporal phases of the current in the vertical control system coils at the ELM occurrence times (t_R, upper panels) and at times just before (t_B, lower panels) with Rayleigh's R values (top left), each panel. The left hand set of panels are for all ELMs that occur in the time interval $t = 6.4$ s–7.1 s of synchronous dynamics in plasma 30416 and confirm strong phase localization in the upper (I_C^u) coils and to a lesser extent, the lower (I_C^l) coils. The right hand set of panels are for all ELMs that occur in a time interval of equal duration before the transition to synchronous dynamics, $t = 5.5$ s–6.2 s.

oscillations coinciding with the occurrence times of *all* the natural ELMs. In such a synchronous state, continual nonlinear feedback between global plasma dynamics and control system is intrinsic to natural ELMing.

ELMs can also be triggered externally. One method is to modify the conditions at the edge by injecting quickly ionizing frozen deuterium pellets.[15–17] Toroidally nonuniform magnetic perturbations also can modify ELMs.[18–20] Externally applied vertical magnetic kicks[9–12] are used to pace ELMs, they exert a force on the large toroidal current carried by the plasma which induces vertical plasma motion. These vertical magnetic kicks are induced by pulsing the current in the same vertical stabilization field coils, discussed here, that are used by the control system to regulate the plasma. In particular (see, for example, Fig. 8 of Ref. 12), kick experiments that can scan a range of kick frequencies find that the more closely the kick frequency approaches the

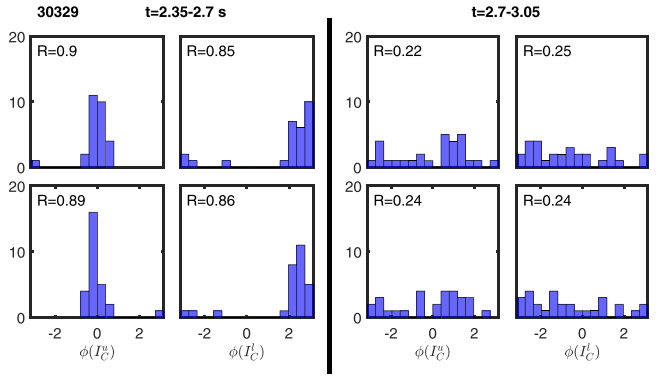

FIG. 12. Each set of four panels plots histograms of instantaneous temporal phases of the current in the vertical control system coils at the ELM occurrence times (t_R, upper panels) and at times just before (t_B, lower panels) with Rayleigh's R values (top left), each panel. The left hand set of panels are for all ELMs that occur in the time interval $t = 2.35 - 2.7$ s of synchronous dynamics in plasma 30930 and confirm strong phase localization in both the upper (I_C^u) coils and the lower (I_C^l) coils. The right hand set of panels are for all ELMs that occur in a time interval of equal duration after the end of the interval of synchronous dynamics, $t = 2.7$ s–3.05 s.

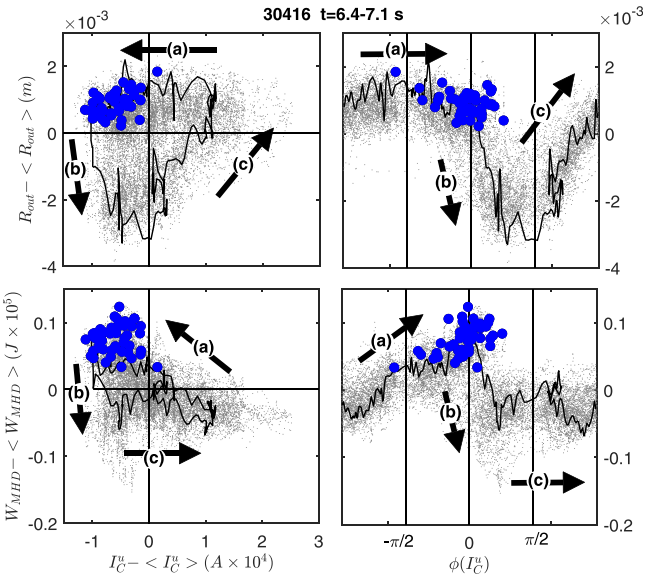

FIG. 13. Vertical control system current phase orders ELM cycle dynamics in plasma 30416. The mean subtracted location of the plasma outer edge (upper panels) and the total plasma MHD energy (lower panels) are plotted versus the mean subtracted current in the control system field coils (left panels) and its phase (right panels). The signals are plotted for the full interval of synchronous dynamics $t = 6.4 - 7.1$ s (grey dots). One cycle of this dynamics, from one ELM to the next, is overplotted (solid black line). All ELMs occurring in $t = 6.4 - 7.1$ s are shown; for each ELM, the signals at the time t_B just before ELM onset are plotted (blue filled circles). The dynamics is a build up phase (a) terminating in ELM onset, followed by the ELM crash (b) and recovery (c).

frequency of natural ELMing, the smaller the kick amplitude required to trigger ELMs. This is consistent with *entrainment* where the ELMs are forced, or entrained, to occur at the kick frequency. It raises the possibility of a resonant interaction

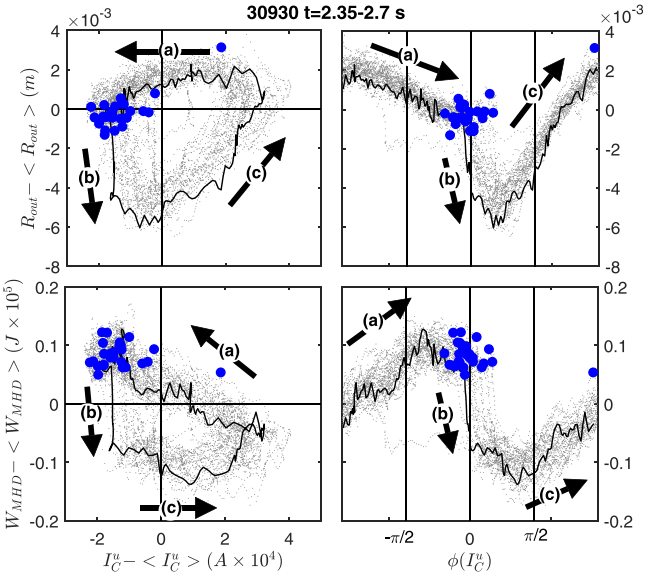

FIG. 14. Vertical control system current phase orders ELM cycle dynamics in plasma 30930. The format is the same as in the previous figure. The signals are plotted for the full interval of synchronous dynamics $t = 2.35$–2.7 s. One cycle of this dynamics, from one ELM to the next, is overplotted (solid black line). All ELMs occurring in $t = 2.35$–2.7 s are shown; for each ELM, the signals at the time t_B just before ELM onset are plotted (blue filled circles). The dynamics is a build up phase (a) terminating in ELM onset, followed by the ELM crash (b) and recovery (c).

between control system and plasma. This possibility was then explored on JET by Ref. 35 who as in Refs. 29–31 found the "simplest and clearest evidence" for the involvement of the control system in natural ELMing to be in toroidal full flux loop signals. In addition[35] identified vertical displacements, consistent with a mechanism analogous to the magnetic kick experiments.

Resonant instability is a fundamental aspect of active feedback control (for a simple mechanical example see Ref. 36). If the control system has an unstable region of its frequency response and if the ELMs happen to naturally occur at this resonant frequency of the control system or one of its harmonics, then the control system will sympathetically oscillate at large amplitude with the ELM cycle and one will see phase correlation. The ASDEX Upgrade control system is specifically designed to suppress known plasma instabilities.[27] It does this on a fast timescale: "the entire control loop is executed in a base cycle of up to 1 ms duration. This length is given by the response time of ASDEX Upgrade fastest actuator, the power supply for the vertical stabilisation coils."[27] The control system takes as its inputs multiple plasma properties, including parameters inferred from plasma equilibria calculated in real time. Examples of these are the plasma stored energy W_{MHD} and the edge position R_{out} which are at ~50 ms time resolution. There are also possible time-lags in the coupling between control system and plasma. On ASDEX Upgrade, there is passive vertical position control by the passive stabilizing loop (PSL, see Fig. 1 of Ref. 28). The vertical stabilization coils may be too far from the plasma for a fast vertical position correction. Nevertheless, voltage pulse trains applied to these vertical stabilization field coils are capable of achieving kicked or entrained ELMs.

For resonance with the control system to feature in the physics of natural ELMing would require a frequency matching between the natural ELMs and the control system. An estimate of the ELM frequency observed here is given by the average inter-ELM time interval over the time intervals of synchronous dynamics. These are $66.7\,s^{-1}$ and $80\,s^{-1}$ for plasma 30416 and plasma 30930, respectively. Whilst resonance cannot be excluded, it would require quite specific conditions for the plasma and control system.

In contrast, phase synchronization can occur over a broad range of conditions.[24] An exemplar is Huygens' observation that several pendulum clocks placed on a shelf will in time become completely synchronized with each other. This is a physical analogue for systems which can become phase synchronized through the interaction with a mean field or through active feedback from a control system.

Importantly, the elements of synchronized systems, in general, do not execute simple harmonic motion, instead they have limit cycle dynamics. Huygens' clock pendula, for example, slowly lose energy by damping, and then once per cycle, gain energy almost instantaneously from the clock escapement mechanism. Under time reversal, this becomes integrate-and-fire dynamics, which is also a central characteristic of the natural ELM cycle: the system slowly gains total energy which it then releases during the ELM on a fast timescale. It has been found that "regardless of the ratio between the pendulum frequency and the natural frequency of the platform, both synphaseous and antiphaseous motions of the pendulums are stable" [Ref. 37, p. 154]. Huygens' clocks are found experimentally to phase synchronize when placed on a bench that is free to move, or on a solidly anchored house beam. Phase synchronization thus encompasses rich dynamics. Huygens' clocks are still an active area of research with dynamics including period doubling and the bifurcation route to chaos.[38] Key properties, such as the frequency of synchronous dynamics, emerge from the coupled system and can be different to those of the individual elements: Huygens' clocks on the shelf can become slow.[39]

Further work that explores a wider range of plasma conditions is needed to determine over what range of ELM frequencies synchronization can occur. In particular, during intervals of synchronous dynamics, the phase relationship found in the control system field coils should hold even if the ELM frequency is drifting. An informative experiment would be to see if the plasma could be continually maintained in a synchronous state with fixed phase relationship, whilst plasma conditions are slowly changed to sweep the ELM frequency. This might distinguish between different physical scenarios.

VII. CONCLUSIONS

We report observational support for a new hypothesis[29–32] that naturally occurring ELMs can result from phase coherent nonlinear feedback between plasma and the control system that is required to stabilize the plasma. We suggest that this is an example of phase synchronization; it involves phase coherent feedback and is a distinct mechanism from that of the entrainment of triggered ELMs by externally applied vertical magnetic kicks[9–12] which relies on kicks of sufficiently large amplitude, typically much larger than that seen in the control system vertical field coil current during natural ELMing. The vertical control coil current phase may provide a parameter that orders ELM cycle dynamics even if the ELM frequency is drifting. On JET, we found a class of prompt[29–32] natural ELMs that occur at a specific phase of the plasmas own response to the previous ELM. We would thus expect under some plasma conditions a global dynamics where *all* the ELMs are "prompt" with each ELM directly following the previous one. We have identified just such a dynamics here on ASDEX Upgrade in which the excursions of the control system and perturbations in the plasma are completely phase synchronized,[24–26] with their synchronous oscillations coinciding with the occurrence times of *all* the natural ELMs. In such a synchronous state, continual nonlinear feedback between global plasma dynamics and control system is intrinsic to natural ELMing.

When there is fully synchronous dynamics, the ELM occurrence times and energies become more predictable with ELMs naturally occurring at a specific phase of the vertical control coil current and with a frequency which is an emergent property of the non-linearly coupled control system and plasma. This may provide real-time operational information on the likelihood of ELM occurrence, suggesting mitigation

strategies in which the vertical control system phase is used to modify natural ELMs. It suggests the possibility that in these fully synchronous states the coupled plasma, control system, and environment, taken as a single system, could be tuned to give natural ELMing at a frequency which in turn may lead to more benign levels of peak heat load to plasma facing components.

ACKNOWLEDGMENTS

This project received funding from the European Union's Horizon 2020 research and innovation programme under Grant Agreement No. 210130335 and from the RCUK Energy Programme [Grant No. EP/P012450/1]. The views and opinions expressed herein do not necessarily reflect those of the European Commission. S.C.C. acknowledges a Fulbright-Lloyd's of London Scholarship and AFOSR Grant No. FA9550-17-1-0054.

[1]F. Wagner, Plasma Phys. Controlled Fusion **49**, B1–B33 (2007).
[2]H. Zohm, Plasma Phys. Controlled Fusion **38**, 105–128 (1996).
[3]A. Loarte, G. Saibene, R. Sartori, D. Campbell, M. Becoulet, L. Horton, T. Eich, A. Herrmann, G. Matthews, N. Asakura, A. Chankin, A. Leonard, G. Porter, G. Federici, G. Janeschitz, M. Shimada, and M. Sugihara, Plasma Phys. Controlled Fusion **45**, 1549 (2003).
[4]K. Kamiya, N. Asakura, J. Boedo, T. Eich, G. Federici, M. Fenstermacher, K. Finken, A. Herrmann, J. Terry, A. Kirk *et al.*, Plasma Phys. Controlled Fusion **49**, S43–S62 (2007).
[5]A. W. Leonard, Phys. Plasmas **21**, 090501 (2014).
[6]M. Shimada, D. J. Campbell, V. Mukhovatov, M. Fujiwara, N. Kirneva, K. Lackner, M. Nagami, V. D. Pustovitov, N. Uckan, J. Wesley *et al.*, Nucl. Fusion **47**, S1–S17 (2007).
[7]R. J. Hawryluk, D. J. Campbell, G. Janeschitz, P. R. Thomas, R. Albanese, R. Ambrosino, C. Bachmann, L. Baylor, M. Becoulet, I. Benfatto, J. Bialek, A. Boozer *et al.*, Nucl. Fusion **49**, 065012 (2009).
[8]C. E. Kessel, D. Campbell, Y. Gribov, G. Saibene, G. Ambrosino, R. V. Budny, T. Casper, M. Cavinato, H. Fujieda, R. Hawryluk *et al.*, Nucl. Fusion **49**, 085034 (2009).
[9]Y. Liang, H. R. Koslowski, P. R. Thomas, E. Nardon, B. Alper, P. Andrew, Y. Andrew, G. Arnoux, Y. Baranov, M. Bécoulet *et al.*, Phys. Rev. Lett. **98**, 265004 (2007).
[10]P. T. Lang, A. W. Degeling, J. B. Lister, Y. R. Martin, P. J. Mc Carthy, A. C. C. Sips, W. Suttrop, G. D. Conway, L. Fattorini, O. Gruber, L. D. Horton, A. Herrmann, M. E. Manso, M. Maraschek, V. Mertens, A. Mück, W. Schneider, C. Sihler, W. Treutterer, H. Zohm, and ASDEX Upgrade Team, Plasma Phys. Controlled Fusion **46**, L31 (2004).
[11]E. de la Luna, I. T. Chapman, F. Rimini, P. J. Lomas, G. Saibene, F. Koechl, R. Sartori, S. Saarelma, R. Albanese, and J. Flanagan, Nucl. Fusion **56**, 026001 (2016).
[12]A. W. Degeling, Y. R. Martin, J. B. Lister, L. Villard, V. N. Dokouka, V. E. Lukash, and R. R. Khayrutdinov, Plasma Phys. Controlled Fusion **45**, 1637 (2003).
[13]T. E. Evans, R. A. Moyer, K. H. Burrell, M. E. Fenstermacher, I. Joseph, A. W. Leonard, T. H. Osborne, G. D. Porter, M. J. Schaffer, P. B. Snyder, P. R. Thomas, J. G. Watkins, and W. P. West, Nat. Phys. **2**, 419 (2006).
[14]A. Kirk, J. Harrison, Y. Liu, E. Nardon, I. T. Chapman, and P. Denner, Phys. Rev. Lett. **108**, 255003 (2012).
[15]L. R. Baylor, N. Commaux, T. C. Jernigan, N. H. Brooks, S. K. Combs, T. E. Evans, M. E. Fenstermacher, R. C. Isler, C. J. Lasnier, S. J. Meitner *et al.*, Phys. Rev. Lett. **110**, 245001 (2013).
[16]P. T. Lang, G. D. Conway, T. Eich, L. Fattorini1, O. Gruber, S. Günter, L. D. Horton, S. Kalvin, A. Kallenbach, M. Kaufmann, G. Kocsis, A. Lorenz, M. E. Manso, M. Maraschek, V. Mertens, J. Neuhauser, I. Nunes, W. Schneider, W. Suttrop, H. Urano, and ASDEX Upgrade Team, Nucl. Fusion **44**, 665 (2004).
[17]P. T. Lang, J. Neuhauser, L. D. Horton, T. Eich, L. Fattorini, J. C. Fuchs, O. Gehre, A. Herrmann, P. Ignacz, M. Jakobi, S. Kalvin, M. Kaufmann, G. Kocsis, B. Kurzan, C. Maggi, M. E. Manso, M. Maraschek, V. Mertens, A. Mück, H. D. Murmann, R. Neu, I. Nunes, D. Reich, M. Reich, S. Saarelma, W. Sandmann, J. Stober, U. Vogl, and ASDEX Upgrade Team, Nucl. Fusion **43**, 1110 (2003).
[18]T. C. Hender, R. Fitzpatrick, A. W. Morris, P. G. Carolan, R. D. Durst, T. Edlington, J. Ferreira, S. J. Fielding, P. S. Haynes, J. Hugill, I. J. Jenkins, R. J. La Haye, B. J. Parham, D. C. Robinson, T. N. Todd, M. Valovic, and G. Vayakis, Nucl. Fusion **32**, 2091 (1992).
[19]T. E. Evans, R. A. Moyer, P. R. Thomas, J. G. Watkins, T. H. Osborne, J. A. Boedo, E. J. Doyle, M. E. Fenstermacher, K. H. Finken, R. J. Groebner, M. Groth, J. H. Harris, R. J. La Haye, C. J. Lasnier, S. Masuzaki, N. Ohyabu, D. G. Pretty, T. L. Rhodes, H. Reimerdes, D. L. Rudakov, M. J. Schaffer, G. Wang, and L. Zeng, Phys. Rev. Lett. **92**, 235003 (2004).
[20]W. Suttrop, T. Eich, J. C. Fuchs, S. Günter, A. Janzer, A. Herrmann, A. Kallenbach, P. T. Lang, T. Lunt, M. Maraschek, R. M. McDermott, A. Mlynek, T. Ptterich, M. Rott, T. Vierle, E. Wolfrum, Q. Yu, I. Zammuto, and H. Zohm, (ASDEX Upgrade Team), Phys. Rev. Lett. **106**, 225004 (2011).
[21]P. B. Snyder, H. R. Wilson, and X. Q. Xu, Phys. Plasmas **12**, 056115 (2005).
[22]J. W. Connor, Plasma Phys. Controlled Fusion **40**, 531 (1998).
[23]S. Saarelma, A. Alfier, M. N. A. Beurskens, R. Coelho, H. R. Koslowski, Y. Liang, I. Nunes, and JET EFDA Contributors, Plasma Phys. Controlled Fusion **51**, 035001 (2009).
[24]A. Pikovsky, M. G. Rosenblum, and J. Kurths, *Synchronization: A Universal Concept in Nonlinear Sciences* (Cambridge Univ. Press, 2003).
[25]M. G. Rosenblum, A. S. Pikovsky, and J. Kurths, Phys. Rev. Lett. **76**, 1804 (1996).
[26]J. T. C. Schwabedal and A. S. Pikovsky, Phys. Rev. Lett. **110**, 204102 (2013).
[27]W. Treutterer, R. Cole, K. Lüddecke, G. Neu, C. Rapson, G. Raupp, D. Zasche, T. Zehetbauer, and ASDEX Upgrade Team, Fusion Eng. Des. **89**, 146 (2014).
[28]L. Giannone, M. Reich, M. Maraschek, E. Poli, C. Rapson, L. Barrera, R. McDermott, A. Mlynek, Q. Ruan, W. Treutterer *et al.*, Fusion Eng. Des. **88**, 3299 (2013).
[29]S. C. Chapman, R. O. Dendy, A. J. Webster, N. W. Watkins, T. N. Todd, J. Morris, and JET-EFDA Contributors, in *Proceedings of 41st EPS Conference on Plasma Physics, Europhysics Conference Abstracts* (European Physical Society, 2014), Vol. 38F, ISBN 2-914771-90-8, Paper No. 101.
[30]S. C. Chapman, R. O. Dendy, T. N. Todd, N. W. Watkins, A. J. Webster, F. A. Calderon, and J. Morris, Phys. Plasmas **21**, 062302 (2014).
[31]S. C. Chapman, R. O. Dendy, T. N. Todd, N. W. Watkins, F. A. Calderon, J. Morris, and JET Contributors, Phys. Plasmas **22**, 072506 (2015).
[32]S. C. Chapman, R. O. Dendy, P. T. Lang, N. W. Watkins, F. Calderon, M. Romanelli, T. N. Todd, and JET Contributors, Nucl. Fusion **57**, 022017 (2017).
[33]S. C. Chapman, P. T. Lang, R. O. Dendy, L. Giannone, N. W. Watkins, ASDEX Upgrade Team, and Eurofusion MST Team, in Proceedings of 44th EPS Conference on Plasma Physics (2017), Vol. 41F, ISBN: 979-10-96389-07.
[34]N. I. Fisher, Statistical Analysis of Circular Data Revised edition CUP (1995).
[35]A. J. Webster, J. Morris, T. N. Todd, S. Brezinsek, P. Coad, J. Likonen, M. Rubel, and JET EFDA Contributors, Phys. Plasmas **22**, 082501 (2015).
[36]R. Smith, Changing the Effective Mass to Control Resonance Problems, Sound and Vibration, May 2001, pp. 14–17.
[37]I. I. Blekhman, *Synchronization in Science and Technology* (Translated by E. I. Rivin) (ASME Press, New York, NY, 1988).
[38]A. R. Willms, P. M. Kitanov, and W. F. Langford, R. Soc. Open Sci. **4**, 170777 (2017).
[39]J. P. Ramirez, L. A. Olvera, H. Nijmeijer, and J. Alvarez, Sci. Rep. **6**, 23580 (2016).